Article

Concomitant Chemoradiation Therapy with Gold Nanoparticles and Platinum Drugs Co-Encapsulated in Liposomes

Gabriel Charest [1,*], **Thititip Tippayamontri** [1,2], **Minghan Shi** [1], **Mohamed Wehbe** [3],
Malathi Anantha [3], **Marcel Bally** [3] **and Léon Sanche** [1]

[1] Department of Nuclear Medicine and Radiobiology and Medical Research Center,
Faculty of Medicine and Health Sciences, Université de Sherbrooke, Sherbrooke, QC J1H 5N4, Canada;
Thititip.T@chula.ac.th (T.T.); Minghan.Shi@USherbrooke.ca (M.S.); Leon.Sanche@usherbrooke.ca (L.S.)

[2] Department of Radiological Technology and Medical Physics, Chulalongkorn University,
Bangkok 10330, Thailand

[3] British Columbia Cancer Agency (BCCA), Vancouver, BC V6H 3Z6, Canada; mwehbe@bccrc.ca (M.W.);
manantha@bccrc.ca (M.A.); mbally@bccrc.ca (M.B.)

* Correspondence: Gabriel.Charest@Usherbrooke.ca

check for
updates

Abstract: A liposomal formulation of gold nanoparticles (GNPs) and carboplatin, named LipoGold, was produced with the staggered herringbone microfluidic method. The radiosensitizing potential of LipoGold and similar concentrations of non-liposomal GNPs, carboplatin and oxaliplatin was evaluated in vitro with the human colorectal cancer cell line HCT116 in a clonogenic assay. Progression of HCT116 tumor implanted subcutaneously in NU/NU mice was monitored after an irradiation of 10 Gy combined with either LipoGold, GNPs or carboplatin injected directly into the tumor by convection-enhanced delivery. Radiosensitization by GNPs alone or carboplatin alone was observed only at high concentrations of these compounds. Furthermore, low doses of carboplatin alone or a combination of carboplatin and GNPs did not engender radiosensitization. However, the same low doses of carboplatin and GNPs administered simultaneously by encapsulation in liposomal nanocarriers (LipoGold) led to radiosensitization and efficient control of cell proliferation. Our study shows that the radiosensitizing effect of a combination of carboplatin and GNPs is remarkably more efficient when both compounds are simultaneously delivered to the tumor cells using a liposomal carrier.

1. Introduction

The necessity to protect healthy tissues surrounding a tumor is a major issue in radiotherapy and limits the therapeutic radiation dose. A promising avenue to increase this dose, while decreasing collateral damage consists of developing radiosensitizers or radio-enhancers that increase relative biological effectiveness (RBE) at the tumor [1,2]. In principle, such treatment could be optimized by injecting the radiosensitizer directly into the tumor together with a chemotherapeutic agent. In this case, the detrimental effects of increased radiation dose and chemotherapy would be much more localized at the tumor. Based on recent advances in molecular radiation physics, we show in this article that such a combination may offer an interesting alternative application of chemoradiation therapy. We suggest encapsulating in liposomes both a gold nanoparticle (GNP) to enhance the local dose and a Pt drug to act as a chemotherapeutic agent (CA). The GNPs supply a high density of short-range low

energy electrons (LEEs), which strongly and locally react with the Pt-CA bound to vital biomolecules, such as DNA.

When X-rays interact with a gold nanoparticle (GNP), LEEs are emitted in large numbers [3–5]. The electron emission coefficient is larger by roughly two orders of magnitude in the 10–80 keV range, compared to that of biological tissue [6]. The electron energy distribution extends from a few eV to energies close to the primary photon energy [4,7,8]. Considering the range of electrons in water and the spherical geometrical factor, most of the LEE density lies within submicrometer distances from the surface of a GNP irradiated with such X-rays [9]. Electrons with energies above the ionization potential of the medium produce a further generation of LEEs. Electrons of energy below 30 eV (i.e., LEEs) are the most numerous reactive species created around the GNP and carry a large portion of the energy absorbed by the metal [7,8,10]. Thus, GNPs are essential generators of LEEs, which have extremely short ranges and can confine, within the nanometer range, damages created by ionizing radiation (IR). Furthermore, a different mechanism of radiolysis, related to the production of hydroxyl radicals in the presence of GNPs in solution, has been shown to contribute to their radiosensitizing properties [11].

LEEs strongly react with the surrounding medium, mainly via a resonant interaction, which leads to their temporary capture by a molecule or a moiety of a large biomolecule, near the GNP. This leads to the formation of a molecular transient anions (TAs) [12]. TAs can decay by reemitting the captured electron (i.e., autoionization) or by dissociation (i.e., dissociative electron attachment). Since autoionization can leave the molecule in a dissociative electronic state, both channels can efficiently break bounds and damage biomolecules [12]. The type of damages induce by LEEs in DNA has been analyzed in detail by various techniques. It includes, base damage and cleavage, single and double strand breaks and other clustered lesions, consisting of strand breaks and base damages [11,13–16]. Similar damages were observed and enhanced when GNPs were bound to DNA [17–20].

Recent investigations of the action of LEEs with the types of Pt-DNA complexes formed during radiotherapy in the nucleus of cells have demonstrated that the platinum-based chemotherapeutic agents (Pt-CAs) cisplatin, oxaliplatin, and carboplatin increase two- to three-fold the damage induced by LEEs, causing higher levels of potentially lethal lesions including cluster damages [21,22]. Furthermore, the energy required for LEEs to induce cluster damage to DNA was found to be much lower when the Pt-CAs were bound to DNA [22].

The enhancement of radiation damage and the biological effects, associated with the individual physical and chemical properties of Pt-CAs and GNPs, have been observed in several in vitro and in vivo studies [23–36]. However, from the results obtained individually with GNPs and Pt-CAs, it became obvious that combining both radiosensitizers in a common carrier could considerably enhance the benefit of chemoradiation therapy (i.e., GNPs produce large quantities of LEEs that would strongly react with any Pt-CAs bound to DNA or other biomolecules vital for cell survival). When Pt-CAs or GNPs were bound separately to DNA, high-energy radiation damage was found to increase by factors of 2–4 [18–20]. However, when both GNPs and Pt-CAs were bound to DNA and subjected to the same experimental conditions, DNA double strand breaks increased by a factor of 7.5 [37]. This last observation led to the present in vitro and in vivo experiments to evaluate the anti-cancer potential of this combination. In the present study, we assess the synergy between 80-keV X-ray irradiation and GNPs administered together with Pt-CAs to cancer cells and malignant tumors. To increase the probability of local combination of GNPs and Pt-CAs within tumoral tissue, we produced a liposomal vehicle named LipoGold that can efficiently deliver both compounds simultaneously to tumor cells. The HCT116 human colorectal cancer cell line was used for in vitro clonogenic experiments with carboplatin and oxaliplatin as the CA. Tumor response was determined in immunodeficient NU/NU nude mice with carboplatin as the CA. According to recent results, the limitation of radiotherapy in colorectal cancer treatment [25] could be improved through the use of a liposomal formulation carrying both a CA and radio enhancer. Preliminary results are concisely presented in this article on this novel method of combining metal nanoparticles with CAs in an effort to enhance the benefits of

concomitant chemoradiation therapy. They are provided for various combinations of CA, GNP, and dose of X-ray radiation.

2. Results and Discussions

2.1. Clonogenic Assays

Figure 1 shows the cytotoxicity of HCT116 cells for five different treatments (carboplatin, GNP, GNP + carboplatin, LipoGold, oxaliplatin and GNP + oxaliplatin) at different relative concentrations, with or without a fixed X-ray dose of 2 Gy. The mean survival fraction (SF) for all groups are relative to the control group (CTRL, column 3), which is normalized to 1. For the groups treated without irradiation: The low dose carboplatin [0.144 μg/mL] group (column 1) and the combination of GNPs [1.106 μg/mL] plus carboplatin [0.144 μg/mL] group (column 2) have a SF higher than the control group (CTRL, column 3) LipoGold (column 4), that contains the same concentrations as the bare products (GNPs [1.106 μg/mL] and carboplatin [0.144 μg/mL] (column 2)), produces a SF barely lower than that of the CTRL ($p = 0.06$). Groups for oxaliplatin [0.3973 μg/mL] (column 5), a high dose of GNPs [100 μg/mL] (column 7), carboplatin [18.262 μg/mL] (column 10) and the combination of GNPs [100 μg/mL] plus oxaliplatin [0.3973 μg/mL] (column 11), have SF between 0.61 and 0.40. The combination of a high dose of GNPs [100 μg/mL] plus carboplatin [18.262 μg/mL] (column 12) has a SF of 0.29.
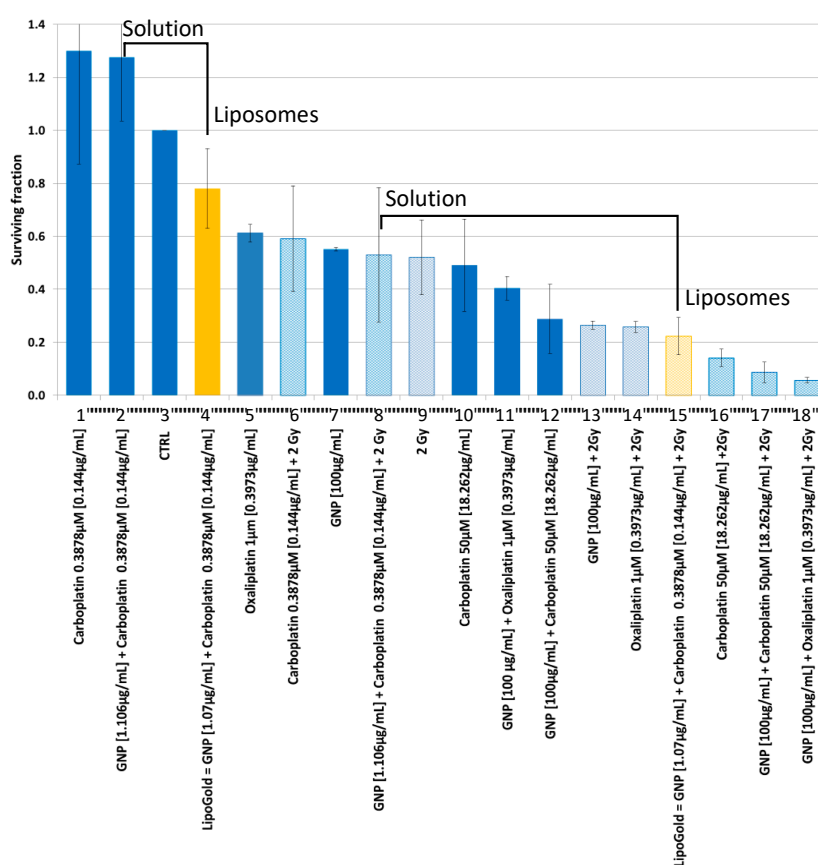

Figure 1. Clonogenic assay with a HCT116 colorectal cancer cell line. Survival fraction after different treatments combined or not with 2 Gy of X-ray radiation of ~80 keV. The measurements were repeated three times for each group. The efficiency of GNPs combined with carboplatin freely dissolved in solution or in liposomal formulation is highlighted.

The groups treated with IR (i.e., the low dose of carboplatin group [0.144 μg/mL] (column 6) and the combination of GNPs [1.106 μg/mL] plus carboplatin [0.144 μg/mL] group (column 8)) have a mean SF, which are slightly higher (but not significantly) than the group treated with radiation

alone (column 9). Groups have a SF between 0.27 and 0.22 include GNPs [100 µg/mL] (column 13), oxaliplatin [0.3973 µg/mL] (column 14) and LipoGold (column 15). SF lower than 0.14 were observed for carboplatin [18.262 µg/mL] (column 16), GNP [100 µg/mL] plus carboplatin [18.262 µg/mL] column 17) and GNP [100 µg/mL] plus oxaliplatin [0.3973 µg/mL] (column 18).

The clonogenic assays (Figure 1) of HCT116 treated with oxaliplatin agrees well with a previous study [38]. Surprisingly, the groups treated with low dose of carboplatin (column 1) or combination of low dose of GNP + carboplatin (column 2) have a higher, but not significant, SF compared to the control group (column 3). A similar ordering is found when IR is combined with these treatments (columns 6, 8) relative to IR alone (column 9). These results suggest that these compounds, at non-lethal doses, could trigger the expression of the repair system that promotes cell survival. However, higher doses of the same compounds without IR (columns 10 and 12) or with IR (columns 16 and 17) do reduce considerably and significantly the SF. Interestingly, when a low dose of GNP + carboplatin are encapsulated in the liposomal formulation LipoGold (column 4), a significant lower SF is observed compared to the free compounds (column 2, $p = 0.046$) and but was not significant compared to the control (column 3, $p = 0.061$). The same pattern is observed when LipoGold is combined with IR (column 15 compared to columns 8 and 9). *The most noteworthy result from this* in vitro *experiment is certainly the demonstration that simultaneous delivery of the compounds by the liposomal formulation is more efficient than the same amount of these compounds without liposomal carrier*. This is clearly seen (annotated in Figure 1) without radiation (column 4 vs. column 2) and with radiation (column 15 vs. column 8).

The stimulation of cell proliferation by a low dose of carboplatin is suspected to be an hormesis phenomenon [39] characterized by a low dose stimulation producing a beneficial response, contrary to a high dose, which would have an inhibitory or toxic effect. In our literature search, we found no specific publication about hormesis due to carboplatin. However, this phenomenon is observed for cisplatin, which has a similar biological action as carboplatin [40].

2.2. In Vivo Antitumoral Efficacy

Figure 2 shows the tumor growth delay after four different treatments (carboplatin, GNP, GNP + carboplatin and LipoGold) at different dosages, with or without X-ray irradiation. The time to reach five times the initial volume of the tumor ±0.2 (5IT) was chosen as a reference point to compare each group. 5IT is also reported in Figure 3. The control group was treated with injection of phosphate buffer saline (column 3) with a 5IT of 9.9 days. No significant difference was observed between PBS (phosphate buffer saline) (column 3), the combination of carboplatin [0.72 µg] plus GNP [5.3 µg] (column 2) and LipoGold (column 4). Only a high dose of carboplatin [0.72 µg] (column 5) shows a small benefit ($p < 0.05$) compared to the PBS group. Interestingly, GNP alone (column 1) shown a faster tumor growth than PBS control ($p < 0.05$). This may be another hormesis phenomenon due to an unknown protective role of low dose of GNP on tumor cell. The same potential protective effect is also observable when we compare carboplatin [0.72 µg] (column 5) to the combination of carboplatin [0.72 µg] plus GNP [5.3 µg] (column 2) ($p < 0.05$). Treatment with radiation alone produces a 5IT of 40.6 days (column 8), but combination of radiation with carboplatin [0.72 µg] + 10 Gy (column 6) or the combination of carboplatin [0.72 µg] plus GNPs [5.3 µg] + 10 Gy (column 7) do not affect the 5IT. LipoGold (carboplatin [0.72 µg] plus GNP [5.3 µg]) + 10Gy (column 9) has a 5IT of 50.4 days. It takes a much higher dose of GNP alone [366.3 µg] than in LipoGold (column 10) to bring 5IT to 53.9 days.

The in vivo tumor growth delay curves of the HCT116 tumor cells implanted in NU/NU nude mice are shown in Figure 2. Each group were compared at the 5IT ± 0.2 (red horizontal highlight) and reported in Figure 3. Small but significant differences were observed for the GNP (column 1) and carboplatin (column 5) groups compared to the control group (column 3), whereas no significant differences were observed for carboplatin + GNP (column 2) and LipoGold (column 4). Similar to the clonogenic assays, when IR is combined to the treatment, low dose of carboplatin (column 6) or carboplatin + GNPs (column 7) do not show significant differences compare to IR alone (column 8). *However, the same low concentration of carboplatin + GNPs in the liposomal formulation a synergistic effect*

occurs, with IR (column 9). High concentration of GNPs + IR (column 10) also enhances radiation therapy. It is interesting to compare the group treated with a low dose of carboplatin + GNPs (column 7) to the LipoGold group (column 9), which received the same concentrations of carboplatin and GNPs in encapsulated form. When these agents were not given in a liposomal formulation, no additional effect appeared, when combined with radiation. On the other hand, the liposomal formulation combined with radiation produces a significant delay on tumor growth. This difference appears to be due to a possible simultaneous cellular incorporation of carboplatin and GNPs, promoted by the liposomal formulation, as opposed to the injection of free carboplatin and GNPs that does not favor colocation in the cell. When a high dose of GNPs is combined to IR (column 10) a 5IT of about 54.75 days is observed. It should be noted that this is a concentration 69 times higher than that of the GNPs in LipoGold (GNPs = [5.3 µg]). The difference in GNP concentration alone cannot explain the difference of only 4 days compared to LipoGold (5IT = 50.35 days).
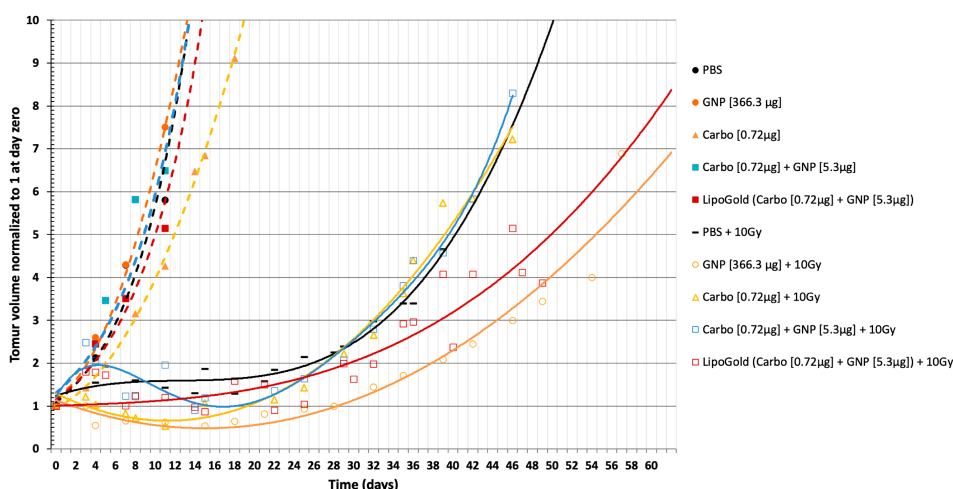

Figure 2. Tumor growth delay for different treatments of Nu/Nu nude mice bearing a subcutaneous HCT116 colorectal cancer cell line. The data passing through the pink horizontal strike-through trace at 5IT ± 0.2 are reported in Figure 3.
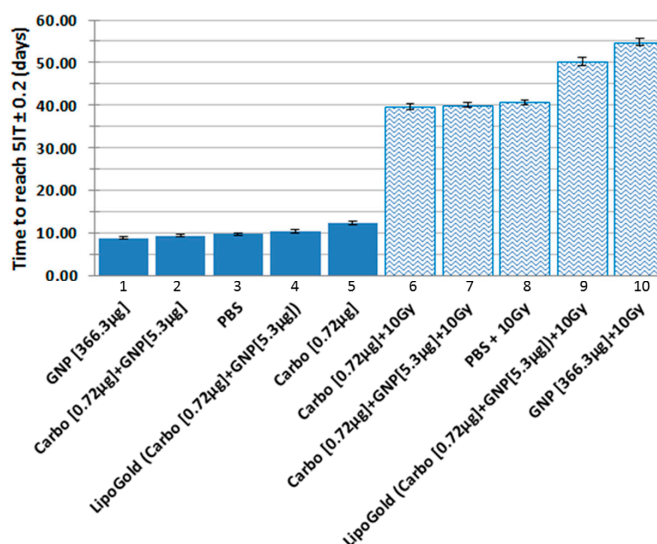

Figure 3. Time to reach five times the initial volume (5IT) after different treatments of Nu/Nu nude mice bearing a subcutaneous HCT116 colorectal cancer cell line. Data from the pink horizontal trace in Figure 2. The SD represent the surviving time passing through the pink line (5IT ± 0.2) of Figure 2.

The mechanistic of incorporation of encapsulated drugs into cells via liposomal transport has been investigated in the literature. Many authors suggest that liposomes are mostly internalized by endocytosis and transported via the endolysosomal pathway [41–43]. Other study suggest direct liposomal fusion to the cell membrane or phagocytosis mechanism [44]. Our hypothesis is that the liposomal formulation will deliver all its load in the same cell allowing cellular colocation of the carried molecules. Presently, we do not know how these pathways combined to provide the much higher efficiency of colocation. Nevertheless, we find the present results to be consistent with our previous in vacuo assays showing that the combination of cisplatin and GNP + IR produces much greater cluster DNA damage compared to cisplatin + IR or GNPs + IR [37].

2.3. Parameters Relevant to Clinical Applications

A resume of publications studying gold nanoparticles combined with radiation is shown in Table 1. Recently, by using about ten times more GNPs than the amount of GNPs contained in LipoGold, we have obtained impressive results with separated injections of GNPs and cisplatin combined with radiation [45]. However, different conditions (radiation doses, cisplatin dose, follow-up time of tumor volume) do not allow perfect comparison with our results. To be clinically relevant, we have evaluated the amount of GNPs of different in vivo studies [25,31,32,45–47] that would correspond to a 60 kg human (last line in Table 1). We found that between 7.14 mg and 20 g of GNPs would have to be used for treatments in patients. With LipoGold, a more realistic in vivo treatment of 1.3 mg of GNP could be delivered via convection-enhanced delivery (CED) to achieve comparable results.

Table 1. Comparison of key publications using gold nanoparticles (GNPs) for cancer treatment studies in relation to injected concentrations of GNPs.

Studies [Ref]	Hainfeld 2004 [32]	Chang 2008 [46]	Hainfeld 2013 [47]	Bobyk 2013 [31]	Shi 2016 [25]	Cui 2017 [45]	This Study	
Tumor type	Mammary carcinoma	Melanoma	Malignant glioma	Glioma	Colorectal cancer	Breast cancer	Colorectal cancer	
Animal model	Mice	Mice	Mice	Rats	Mice	Mice	Mice	
Methods	i.v.	i.v.	i.v.	Convection-enhanced delivery (CED)	Intra tumoral infusion	Intra tumoral infusion	CED (GNP)	CED (LipoGold)
GNP (mg/animal) [1]	35	0.671	80	0.125 to 0.250	0.3663	0.05 to 0.5	0.3663	0.0053
Initial tumor volume (mm^3)	50–90	50 to 90	14.13 to 65.42	33.5	100	250	60	60
Equivalent for human of 60 kg [2] (mg of AuNPs)	8750	167.74	20,000	7.14 to 14.29	91.57	12.5 to 125	91.57	1.325

[1] Assuming weight of mouse and rat of 20 g and 150 g respectively. [2] According to Freireich, E.J. et al., 1966 [48].

3. Materials and Methods

3.1. GNP Production

GNP were produced and stabilized with a thiopronin coating as described by Templeton et al. [49]. Briefly, 0.1033 g of tetrachloroauric acid (Sigma-Aldrich, Oakville, ON, Canada) and 0.1267 g of *N*-(2-mercaptopropionyl) glycerin were dissolved in 11.67 mL of 6:1 methanol: acetic acid. A solution of $NaBH_4$ (0.2 g in 5 mL) was added. The suspension was stirred for 45 min and the solvent was removed by vacuum, purified by dialysis, dried by lyophilization and resuspended in double distillated water to a final concentration of 100 μg/mL. A mean diameter of 2.8 nm for GNPs was measured by transmission electron microscopy (Hitachi H-7500 transmission electron microscope operating at 60–80 kV, 15 μA, 1×10^{-7} Torr). A TEM image of a typical GNP distribution can be found in the on-line Supplementary Materials.

3.2. Liposomal Preparation

Liposomes were produced by the staggered herringbone microfluidic method [50] (NanoAssemblr, Precision NanoSystem, Vancouver, BC, Canada). About 40 different combinations of lipid compositions (50 μmol/mL), aqueous were tried: Lipid ratios and flow rates to determine the best combination for producing LipoGold, which was intended to have a diameter between 100 nm to 140 nm and low polydispersity (lower than 0.2). The ultimate version was produced with a cationic lipid ratio of DOTAP: DSPC: Cholesterol of 45: 6.5: 48.5 with a flow rate of 4 mL/min and an aqueous lipids ratio of 3:1 at 65 °C. The aqueous solution containing GNPs (20 mg/mL) and carboplatin (20 mg/mL) was dissolved in water, whereas the lipid solution (50 μmol/mL) was dissolved in ethanol. To remove any unincorporated therapeutic agent and alcohol, the liposomal solution was purified through a Sephadex^{TM} G-50 column and the cloudy fractions were pooled and purified in a dialysis bag (12–14 kD MWCO) for four days with regular changes of distilled water. Dynamic light scattering (DLS) and polydispersity measurements on the purified liposomes were carried on with a ZETAPALS-Zeta potential Analyzer (Brookhaven instruments, Holtsville, NY, USA). Both measurements were automatically performed by this instrument, from which we could read that the polydispersity was 0.199 ± 0.023. The liposome mean diameter of 134.33 ± 0.27 nm was determined by transmission electron microscopy (Hitachi H-7500 transmission electron microscope operating at 60–80 kV, 15 μA, 1×10^{-7} Torr). A LipoGold TEM image is available in the on-line Supplementary Materials. No trace of ethanol was measured with the alcohol test strips method (ALCO SCREEN, Vista, CA, USA). The liposomal solution (LipoGold) has a final concentration of gold (0.533 mg/mL) and carboplatin (0.072 mg/mL), measured by ICP-MS (X Series II from Thermo Scientific, Waltham, MA, USA). The concentration of carboplatin was the maximum possible to be incorporate in the liposomal formulation with the stock solution (10 mg/mL). The LipoGold formulation, made of cationic lipids [51,52], should be cationic, but the exact Zeta potential was not measured in the present study.

3.3. Cell Culture

HCT116 colorectal carcinoma cell line was obtained from American Type Culture Collection (Manassas, VA, USA). The cells were maintained in Minimum Essential Medium (MEM) (Gibco, NY, USA) containing 10% fetal bovine serum (FBS), 2 mM glutamine, 1 mM Sodium-Pyruvate, 100 units/mL penicillin and 100 μM streptomycin at 37 °C in a humidified atmosphere containing 5% CO_2.

3.4. In Vitro Clonogenic Assays

Triplicates of cells were seeded in completed MEM at a density of 1.0×10^4 cells per well in 96-well plates and incubated for 24 h. Cells were incubated with various drug concentrations in MEM without FBS for 4 h at 37 °C. The cells were irradiated with a Therapax HF150T x-ray source operated at 10.4 mA and 100 kV. The beam was filtered to yield photons with a most probable energy of ~ 80 keV. The dose of 2 Gy was delivered via a cone applicator with a 10 cm diameter at the base and a source to wells distance of 25 cm. Immediately after, cells were rinsed with PBS, trypsinated and plated in P100 petri dishes with complete MEM and incubated at 37 °C, 5% CO_2. Colonies were counted 7 days later.

3.5. In Vivo Antitumoral Activity

Animal experimentations were approved by the Université de Sherbrooke Animal Care and Use Committee (Approval number 235-10). For all procedures (implantation, chemotherapy and radiotherapy), mice were anesthetized with an intraperitoneal injection of ketamine/xylazine (87/13 mg/mL) at 1 mL/kg.

For tumor implantation, HCT116 cells were inoculated (2×10^6 cells in 0.1 mL) subcutaneously (s.c.) into each rear flank area of outbred male NU/NU nude mice at 4–6 weeks of age (*n* = 3–5) (Charles River Laboratories, Saint-Constant, QC, Canada). The tumor volume was measured starting one week post-implantation and then biweekly until treatment. Tumor volumes were calculated with the formula:

$V \ (\text{mm}^3) = \pi/6 \times a \ (\text{mm}) \times b^2 \ (\text{mm}^2)$, where a and b were the largest and smallest perpendicular tumor diameters, respectively.

Chemotherapy treatments began when tumor volume reached a range of 30–60 mm^3. Ten µL of tested solution (carboplatin [72 µg/mL], GNP [36.63 mg/mL], PBS 1X, LipoGold (carboplatin [72 µg/mL], GNP [0.53 mg/mL]) were injected by convection-enhanced delivery (CED) directly into the tumor. Tumor measurements and volume calculations were done 3 times per week until reaching the endpoint of 1 cm^3, followed by euthanasia of the mice. Mice were not monitored for weight considering the problem of the added weight of the growing tumor. However, compared to healthy mice, tumor-bearing mice showed no visual sign of toxicity (loss of activity and grooming, or additional stress) up to the endpoint. No other toxicity analysis was performed.

Tumors were irradiated (10 Gy) 24 h after chemotherapy treatment, using a Therapax HF150T operated at 13.2 mA and 150 kV, equipped with the 1 cm diameter applicator and filter #8 (0.2 mm of aluminum and 1 mm of copper) to yield photons with an average energy of 86 keV. This radiation dose was chosen, because by itself, it induces a partial tumor response, which allowed assessment of the combined effect of chemotherapy with radiation. X-rays of ~80 keV were chosen for their capacity to deliver large quantities of LEEs with a relatively large penetration in tissue. Radiation was applied to both sides of the rear flank, where the tumor was implanted. Note: Experiments using GNP [366.3 µg] were performed by our group and have been published recently [25]. Rough data form [25] were used in the present publication for comparison needs.

3.6. Statistical Analysis

Paired *t*-test adjusted by False Discovery rate (Benjamini-Hochberg) was used to compare each group. Significant difference was inferred by a *p* value less than 0.05. Statistical tables relative to Figures S1 and S3 are found in on-line Supplementary Materials.

4. Conclusions

The preliminary results presented in this paper have allowed investigating the in vitro and in vivo biological response of a wide range of combination of GNPs, X-ray irradiation, carboplatin and a liposomal formulation of carboplatin and GNPs. Now that the most efficient combination has been identified, we hope that our results will incite more elaborate research with the most interesting product (e.g., LipoGold) to fully establish its clinical potential. Among others, such studies should include details on the cellular incorporation of drugs, precise measurements of Zeta potentials and a more quantitative analysis of toxicity, including measurements of body weight changes. We also point out that valuable biological information could be obtained from a more detail analysis of the hormesis phenomenon reported in the present study.

In this study, mice bearing a human colorectal tumor were treated with radiation alone and in various combination of Pt-CA and GNPs administered by CED (i.e., direct low flow injection into the tumor) [53]. The intra-tumoral CED method was chosen because of its capacity to allow for up to hundred times more GNP tumor uptake than intravenous injection [25]. The most effective radiotherapeutic treatment was obtained when carboplatin and GNPs were brought together to the tumor cells via a liposomal carrier prior to irradiation. According to literature, the rationale behind liposomal transportation of CAs is mainly due for their favorable properties, such as biocompatibility, side effect reduction, and preferential tumor accumulation, which are caused by the enhance permeability and retention effect [54]. The present study suggests that in addition to these advantages, liposomal encapsulation could serve to simultaneously co-inject CAs and GNPs to considerably increase the efficiencies of chemoradiation therapy. The conjectured cellular colocation of platinum drugs and GNPs due to their encapsulation seems advantageous to reach a high level of radiosensitization, when only low concentrations of these compounds can be tolerated by the patient. CED of radiosensitizers, such as LipoGold are expected to increase considerably the radiation dose and RBE at the tumor level, while reducing radiation damage to healthy cells.

Although much more information is needed to explain the metabolic and cellular behavior of LipoGold, the present investigation serves as an example of the guidelines that can be provided by fundamental research on the action of IR with biomolecules for the development of new types of treatments in radio-oncology. More precisely, this work and previous literature shows that GNPs can be used for efficient radio-enhancement of superficial tumors (e.g., colorectal cancer). However, to administer a realistic gold concentration in eventual clinical applications, colocalization of metal nanoparticles with a radiosensitizer, such as a platinum drug, appears to be a promising avenue.

5. Patents

US Patent application PCT/CA10/00583 "Compositions Comprising a Radiosensitizer and Anti-Cancer Agent and Methods of Uses Thereof".

Supplementary Materials: Supplementary materials can be found at http://www.mdpi.com/1422-0067/21/14/4848/s1.

Author Contributions: G.C. synthesized and characterized GNPs and liposomal formulation: in vitro and in vivo experiments, data acquisitions, analysis and interpretation; he wrote and revised the manuscript. T.T. and M.S. equally performed some in vitro and in vivo experiments. M.W. and M.A. equally assisted for liposomal formulation production, characterization and experimental data interpretation of liposomal analysis. M.B. was remarkably engaged in liposomal formulation design and characterization. L.S. supervised the project and experimental strategy; he partly wrote and reviewed the manuscript. All authors discussed the results and improved the manuscript. All authors have read and agreed to the published version of the manuscript.

Conflicts of Interest: The authors declare no conflict of interest.

Abbreviations

GNPs	Gold nanoparticles
RBE	Relative biological effectiveness
Pt	Platinum drug
CA	Chemotherapeutic agent
Pt-CAs	Platinum-based chemotherapeutic agents
Pt-DNA	Platinum DNA complexes
DSBs	Double strand breaks
keV	Kilo electron Volt
DOTAP	1,2-dioleoyl-3-trimethylammonium-propane
DSPC	1,2-distearoyl-sn-glycero-3-phosphocholine
SF	Surviving fraction
IR	Ionizing radiation
Gy	Gray (unit of radiation dose deposition)
CED	Convection enhanced delivery

References

1. Wardman, P. Chemical Radiosensitizers for Use in Radiotherapy. *Clin. Oncol.* **2007**, *19*, 397–417. [CrossRef] [PubMed]

2. Pottier, A.; Borghi, E.; Levy, L. Metals as radio-enhancers in oncology: The industry perspective. *Biochem. Biophys. Res. Commun.* **2015**, *468*, 471–475. [CrossRef]

3. Wardlow, N.; Polin, C.; Villagomez-Bernabe, B.; Currell, F. A Simple Model to Quantify Radiolytic Production following Electron Emission from Heavy-Atom Nanoparticles Irradiated in Liquid Suspensions. *Radiat. Res.* **2015**, *184*, 518–532. [CrossRef] [PubMed]

4. McQuaid, H.N.; Muir, M.F.; Taggart, L.E.; McMahon, S.J.; Coulter, J.A.; Hyland, W.B.; Jain, S.; Butterworth, K.T.; Schettino, G.; Prise, K.M.; et al. Imaging and radiation effects of gold nanoparticles in tumour cells. *Sci. Rep.* **2016**, *6*, 19442. [CrossRef] [PubMed]

5. Cho, S.H. TH-C-T-6C-04: Estimation of Tumor Dose Enhancement Due to Gold Nanoparticles During Typical Radiation Treatments: A Preliminary Monte Carlo Study. *Med. Phys.* **2005**, *32*, 2162. [CrossRef]

6. Hubbelle, J.; Seltzer, S. Tables of X-Ray Mass Attenuation Coefficients and Mass Energy-Absorption Coefficients, NIST Standard Reference Database 126 (version 1.0). Available online: https://www.nist.gov/pml/x-ray-mass-attenuation-coefficients (accessed on 31 July 2004).

7. Carter, J.D.; Cheng, N.N.; Qu, Y.; Suarez, G.D.; Guo, T. Nanoscale energy deposition by X-ray absorbing nanostructures. *J. Phys. Chem. B* **2007**, *111*, 11622–11625. [CrossRef]

8. Casta, R.; Champeaux, J.P.; Moretto-Capelle, P.; Sence, M.; Cafarelli, P. Electron and photon emissions from gold nanoparticles irradiated by X-ray photons. *J. Nanoparticle Res.* **2015**, *17*, 3. [CrossRef]

9. McMahon, S.J.; Hyland, W.B.; Muir, M.F.; Coulter, J.A.; Jain, S.; Butterworth, K.T.; Schettino, G.; Dickson, G.R.; Hounsell, A.R.; O'Sullivan, J.M.; et al. Biological consequences of nanoscale energy deposition near irradiated heavy atom nanoparticles. *Sci. Rep.* **2011**, *1*, 18. [CrossRef]

10. Casta, R.; Champeaux, J.P.; Cafarelli, P.; Moretto-Capelle, P.; Sence, M. Model for electron emission of high-Z radio-sensitizing nanoparticle irradiated by X-rays. *J. Nanopartic. Res.* **2014**, *16*, 2480. [CrossRef]

11. Sicard-Roselli, C.; Brun, E.; Gilles, M.; Baldacchino, G.; Kelsey, C.; McQuaid, H.; Polin, C.; Wardlow, N.; Currell, F. A new mechanism for hydroxyl radical production in irradiated nanoparticle solutions. *Small* **2014**, *10*, 3338–3346. [CrossRef]

12. Sanche, L. Low-Energy Electron Interaction with DNA: Bond Dissociation and Formation of Transient Anions, Radicals, and Radical Anions. In *Radical and Radical Ion Reactivity in Nucleic Acid Chemistry*; John Wiley & Sons, Inc.: Hoboken, NJ, USA, 2009; pp. 239–293. ISBN 9780470255582.

13. Zheng, Y.; Sanche, L. Low Energy Electrons in Nanoscale Radiation Physics: Relationship to Radiosensitization and Chemoradiation Therapy. *Rev. Nanosci. Nanotechnol.* **2013**, *2*, 1–28. [CrossRef]

14. Shao, Y.; Dong, Y.; Hunting, D.; Zheng, Y.; Sanche, L. Unified Mechanism for the Generation of Isolated and Clustered DNA Damages by a Single Low Energy (5-10 eV) Electron. *J. Phys. Chem. C* **2017**, *121*, 2466–2472. [CrossRef]

15. Zheng, Y.; Sanche, L. Clustered DNA Damages induced by 0.5 to 30 eV Electrons. *Int. J. Mol. Sci.* **2019**, *20*, 3749. [CrossRef]

16. Dong, Y.; Gao, Y.; Liu, W.; Gao, T.; Zheng, Y.; Sanche, L. Clustered DNA Damage Induced by 2-20 eV Electrons and Transient Anions: General Mechanism and Correlation to Cell Death. *J. Phys. Chem. Lett.* **2019**, *10*, 2985–2990. [CrossRef]

17. Brun, E.; Sanche, L.; Sicard-Roselli, C. Parameters governing gold nanoparticle X-ray radiosensitization of DNA in solution. *Colloids Surf. B Biointerfaces* **2009**, *72*, 128–134. [CrossRef] [PubMed]

18. Zheng, Y.; Cloutier, P.; Hunting, D.J.; Sanche, L. Radiosensitization by gold nanoparticles: Comparison of DNA damage induced by low and high-energy electrons. *J. Biomed. Nanotechnol.* **2008**, *4*, 469–473. [CrossRef]

19. Zheng, Y.; Hunting, D.J.; Ayotte, P.; Sanche, L. Radiosensitization of DNA by gold nanoparticles irradiated with high-energy electrons. *Radiat. Res.* **2008**, *169*, 19–27. [CrossRef] [PubMed]

20. Xiao, F.; Zheng, Y.; Cloutier, P.; He, Y.; Hunting, D.; Sanche, L. On the role of low-energy electrons in the radiosensitization of DNA by gold nanoparticles. *Nanotechnology* **2011**, *22*, 465101. [CrossRef]

21. Rezaee, M.; Hunting, D.J.; Sanche, L. New insights into the mechanism underlying the synergistic action of ionizing radiation with platinum chemotherapeutic drugs: The role of low-energy electrons. *Int. J. Radiat. Oncol. Biol. Phys.* **2013**, *87*, 847–853. [CrossRef]

22. Rezaee, M.; Alizadeh, E.; Cloutier, P.; Hunting, D.J.; Sanche, L. A single subexcitation-energy electron can induce a double-strand break in DNA modified by platinum chemotherapeutic drugs. *Chem. Med. Chem.* **2014**, *9*, 1145–1149. [CrossRef]

23. Charest, G.; Sanche, L.; Fortin, D.; Mathieu, D.; Paquette, B. Optimization of the route of platinum drugs administration to optimize the concomitant treatment with radiotherapy for glioblastoma implanted in the Fischer rat brain. *J. Neurooncol.* **2013**, *115*, 365–373. [CrossRef] [PubMed]

24. Charest, G.; Paquette, B.; Fortin, D.; Mathieu, D.; Sanche, L. Concomitant treatment of F98 glioma cells with new liposomal platinum compounds and ionizing radiation. *J. Neurooncol.* **2010**, *97*, 187–193. [CrossRef] [PubMed]

25. Shi, M.; Paquette, B.; Thippayamontri, T.; Gendron, L.; Guérin, B.; Sanche, L. Increased radiosensitivity of colorectal tumors with intra-tumoral injection of low dose of gold nanoparticles. *Int. J. Nanomed.* **2016**, *11*, 5323–5333. [CrossRef] [PubMed]

26. Chithrani, D.B. Intracellular uptake, transport, and processing of gold nanostructures. *Mol. Membr. Biol.* **2010**, *27*, 299–311. [CrossRef]

27. Yang, C.J.; Chithrani, D.B. Nuclear Targeting of Gold Nanoparticles for Improved Therapeutics. *Curr. Top. Med. Chem.* **2015**, *16*, 271–280. [CrossRef]

28. Yang, C.; Bromma, K.; Sung, W.; Schuemann, J.; Chithrani, D. Determining the Radiation Enhancement Effects of Gold Nanoparticles in Cells in a Combined Treatment with Cisplatin and Radiation at Therapeutic Megavoltage Energies. *Cancers* **2018**, *10*, 150. [CrossRef]

29. Tippayamontri, T.; Kotb, R.; Paquette, B.; Sanche, L. Efficacy of cisplatin and lipoplatin^{TM} in combined treatment with radiation of a colorectal tumor in nude mouse. *Anticancer Res.* **2013**, *33*, 3005–3014.

30. Tippayamontri, T.; Kotb, R.; Paquette, B.; Sanche, L. Cellular uptake and cytoplasm/DNA distribution of cisplatin and oxaliplatin and their Liposomal formulation in human colorectal cancer cell HCT116. *Investig. New Drugs* **2011**, *29*, 1321–1327. [CrossRef]

31. Bobyk, L.; Edouard, M.; Deman, P.; Vautrin, M.; Pernet-Gallay, K.; Delaroche, J.; Adam, J.F.; Estève, F.; Ravanat, J.L.; Elleaume, H. Photoactivation of gold nanoparticles for glioma treatment. *Nanomed. Nanotechnol. Biol. Med.* **2013**, *9*, 1089–1097. [CrossRef]

32. Hainfeld, J.F.; Slatkin, D.N.; Smilowitz, H.M. The use of gold nanoparticles to enhance radiotherapy in mice. *Phys. Med. Biol.* **2004**, *49*, 309–315. [CrossRef]

33. Hainfeld, J.F.; Dilmanian, F.A.; Slatkin, D.N.; Smilowitz, H.M. Radiotherapy enhancement with gold nanoparticles. *J. Pharm. Pharmacol.* **2008**, *60*, 977–985. [CrossRef] [PubMed]

34. Hainfeld, J.F.; Dilmanian, F.A.; Zhong, Z.; Slatkin, D.N.; Kalef-Ezra, J.A.; Smilowitz, H.M. Gold nanoparticles enhance the radiation therapy of a murine squamous cell carcinoma. *Phys. Med. Biol.* **2010**, *55*, 3045–3059. [CrossRef] [PubMed]

35. Jain, S.; Coulter, J.A.; Hounsell, A.R.; Butterworth, K.T.; McMahon, S.J.; Hyland, W.B.; Muir, M.F.; Dickson, G.R.; Prise, K.M.; Currell, F.J.; et al. Cell-Specific Radiosensitization by gold nanoparticles at megavoltage radiation energies. *Int. J. Radiat. Oncol. Biol. Phys.* **2011**, *79*, 531–539. [CrossRef] [PubMed]

36. Liu, C.-J.; Wang, C.-H.; Chen, S.-T.; Chen, H.-H.; Leng, W.-H.; Chien, C.-C.; Wang, C.-L.; Kempson, I.M.; Hwu, Y.; Lai, T.-C.; et al. Enhancement of cell radiation sensitivity by pegylated gold nanoparticles. *Phys. Med. Biol.* **2010**, *55*, 931–945. [CrossRef]

37. Zheng, Y.; Sanche, L. Gold nanoparticles enhance DNA damage induced by anti-cancer drugs and radiation. *Radiat. Res.* **2009**, *172*, 114–119. [CrossRef] [PubMed]

38. Tippayamontri, T.; Kotb, R.; Paquette, B.; Sanche, L. Synergism in concomitant chemoradiotherapy of cisplatin and oxaliplatin and their liposomal formulation in the human colorectal cancer HCT116 model. *Anticancer Res.* **2012**, *32*, 4395–4404. [PubMed]

39. Mattson, M.P. Hormesis defined. *Ageing Res. Rev.* **2008**, *7*, 1–7. [CrossRef]

40. Reynolds, A.R. Potential relevance of bell-shaped and u-shaped dose-responses for the therapeutic targeting of angiogenesis in cancer. *Dose Response* **2010**, *8*, 253–284. [CrossRef] [PubMed]

41. Chithrani, D.B.; Dunne, M.; Stewart, J.; Allen, C.; Jaffray, D.A. Cellular uptake and transport of gold nanoparticles incorporated in a liposomal carrier. *Nanomed. Nanotechnol. Biol. Med.* **2010**, *6*, 161–169. [CrossRef] [PubMed]

42. Straubinger, R.M.; Hong, K.; Friend, D.S.; Papahadjopoulos, D. Endocytosis of liposomes and intracellular fate of encapsulated molecules: Encounter with a low pH compartment after internalization in coated vesicles. *Cell* **1983**, *32*, 1069–1079. [CrossRef]

43. Lee, K.D.; Nir, S.; Papahadjopoulos, D. Quantitative Analysis of Liposome-Cell Interactions in Vitro: Rate Constants of Binding and Endocytosis with Suspension and Adherent J774 Cells and Human Monocytes. *Biochemistry* **1993**, *32*, 889–899. [CrossRef] [PubMed]

44. Boulikas, T. Molecular mechanisms of cisplatin and its liposomally encapsulated form, Lipoplatin^{TM}. Lipoplatin^{TM} as a chemotherapy and antiangiogenesis drug. *Cancer Ther.* **2007**, *5*, 351–376.

45. Cui, L.; Her, S.; Dunne, M.; Borst, G.R.; De Souza, R.; Bristow, R.G.; Jaffray, D.A.; Allen, C. Significant Radiation Enhancement Effects by Gold Nanoparticles in Combination with Cisplatin in Triple Negative Breast Cancer Cells and Tumor Xenografts. *Radiat. Res.* **2017**, *187*, 147–160. [CrossRef] [PubMed]

46. Chang, M.Y.; Shiau, A.L.; Chen, Y.H.; Chang, C.J.; Chen, H.H.; Wu, C.L. Increased apoptotic potential and dose-enhancing effect of gold nanoparticles in combination with single-dose clinical electron beams on tumor-bearing mice. *Cancer Sci.* **2008**, *99*, 1479–1484. [CrossRef] [PubMed]

47. Hainfeld, J.F.; Smilowitz, H.M.; O'Connor, M.J.; Dilmanian, F.A.; Slatkin, D.N. Gold nanoparticle imaging and radiotherapy of brain tumors in mice. *Nanomedicine (Lond.)* **2013**, *8*, 1601–1609. [CrossRef]

48. Freireich, E.J.; Gehan, E.A.; Rall, D.P.; Schmidt, L.H.; Skipper, H.E. SQuantitative comparison of toxicity of anticancer agents in mouse, rat, hamster, dog, monkey, and man. *Cancer Chemother. Rep.* **1966**, *50*, 219–244.

49. Templeton, A.C.; Chen, S.; Gross, S.M.; Murray, R.W. Water-Soluble, Isolable Gold Clusters Protected by Tiopronin and Coenzyme A Monolayers. *Langmuir* **1999**, *15*, 66–76. [CrossRef]

50. Zhigaltsev, I.V.; Belliveau, N.; Hafez, I.; Leung, A.K.K.; Huft, J.; Hansen, C.; Cullis, P.R. Bottom-up design and synthesis of limit size lipid nanoparticle systems with aqueous and triglyceride cores using millisecond microfluidic mixing. *Langmuir* **2012**, *28*, 3633–3640. [CrossRef]

51. CD Bioparticles CliposTM Cationic DOTAP Liposomes. Available online: https://www.cd-bioparticles.net/p/5995/clipossuptm-sup-cationic-dotap-liposomes (accessed on 1 July 2020).

52. Campbell, R.B.; Balasubramanian, S.V.; Straubinger, R.M. Influence of cationic lipids on the stability and membrane properties of paclitaxel-containing liposomes. *J. Pharm. Sci.* **2001**, *90*, 1091–1105. [CrossRef]

53. Mehta, A.M.; Sonabend, A.M.; Bruce, J.N. Convection-Enhanced Delivery. *Neurotherapeutics* **2017**, *14*, 358–371. [CrossRef]

54. Maeda, H.; Sawa, T.; Konno, T. Mechanism of tumor-targeted delivery of macromolecular drugs, including the EPR effect in solid tumor and clinical overview of the prototype polymeric drug SMANCS. *J. Control. Release* **2001**, *74*, 47–61. [CrossRef]